Microchemical Journal 196 (2024) 109640

Contents lists available at ScienceDirect

Microchemical Journal

journal homepage: www.elsevier.com/locate/microc

Paper-based biomimetic test-strip for CA15-3 with coloured readout

Mariana C.C.G. Carneiro [a,b], Lígia R. Rodrigues [b], Felismina Moreira [a,b], M. Goreti F. Sales [b,c,*]

[a] BioMark sensor research@ISEP-CEB, School of Engineering, Polytechnic Institute, Porto, Portugal
[b] CEB-LABBELS, Centre of Biological Engineering & Associate Laboratory, Minho University, Braga, Portugal
[c] BioMark sensor research@UC-CEB, Faculty of Sciences and Technology, University of Coimbra, Coimbra, Portugal

ARTICLE INFO

Keywords:
Molecularly imprinted polymer
Biomimetic enzyme-linked immunosorbent assay
Point-of-care
Cellulose paper
Cancer antigen 15–3
Protein biomarker

ABSTRACT

The combination of molecularly-imprinted polymers (MIPs) on paper substrates for capturing a cancer antigen 15–3 (CA15-3) with the traditional coloured transduction scheme of enzyme-linked immunosorbent assay (ELISA) using 3,3′,5,5′-tetramethylbenzidine (TMB), horseradish peroxidase (HRP) and H_2O_2 is presented here for the first time.

Here, the paper surface was modified with a silane derivative containing an amine function that allows subsequent binding of 3-aminophenylboronic acid (3-APBA). The target protein, CA15-3, was then bound via the boronic groups of APBA. The empty space around CA15-3 was filled by polymerization of dopamine. Finally, the CA15-3 template was removed by breaking the imine function to create vacant sites for which CA15-3 has a high affinity. Binding of CA15-3 was detected by oxidation of TMB substrate by HRP in the presence of H_2O_2.

The results showed that the MIP was able to selectively recognize CA15-3 within 3–500 U mL^{-1}, even in complex samples. Quantitative data were extracted by analysing the colour coordinates of images captured with a smartphone using ImageJ. This selective behaviour was confirmed by comparison with a control material (non–polymer, NIP).

Overall, the described approach has advantages over conventional ELISA, namely low cost and high stability, which is due to the use of MIP as a trapping element acting as a selective pre-concentration point of CA15-3. To our knowledge, this is the first biomimetic ELISA (B-ELISA) on paper substrate used for macromolecules such as proteins. We believe that this approach has the potential to be applied to other protein disease biomarkers, making it a suitable tool for screening glycoproteins at the point-of-care.

1. Introduction

Glycoproteins are involved in important biological processes such as molecular recognition, cell signalling, immune response, and control of cell development. Abnormal expression of glycoproteins is generally associated with the occurrence of many diseases [1]. Thus, these molecules can be used as both target biomarkers and therapeutics [2], and their monitoring is essential.

Cancer antigen 15–3 (CA15-3) is the soluble form of mucin 1 (MUC-1) [3] with ≈400 kDa. It is overexpressed in 90 % of breast cancer cases [4,5] being the most widely used biomarker in serum of patients with breast cancer [3]. Several biosensors were already reported for CA15-3 detection, in which different recognition elements as antibodies [6–8], MIPs [9–11] or aptamers [12] were coupled with electrochemical [7–9,11] or optical [6,12,13] signal transduction approaches.

The enzyme-linked immunosorbent assay (ELISA) is the gold standard for monitoring various glycoprotein-based biomarkers. It offers high sensitivity and selectivity [14], but is time-consuming and requires expensive reagents and specialised equipment for analysis that is not portable. It also produces hazardous waste. All these characteristics are unsuitable for point-of-care analysis, which would be of great importance in the clinical context.

Scientists tried to overcome the disadvantages of the traditional ELISA by replacing the traditional 96-well plate with cellulose paper substrates and developed the paper-based ELISA (P-ELISA) [15]. The P-ELISA combines the high selectivity and sensitivity of the traditional ELISA with the advantages of using a renewable substrate. Cellulose is also flexible, portable, and inexpensive. Its capillary action enables rapid procedures, which, together with its porous structure, facilitates reagent storage [16–18]. The P-ELISA can be performed in less than one hour and consumes only small amounts of samples and reagents (1–10 μL), which reduces the time and cost of the test. Therefore, it is a suitable

* Corresponding author at: Faculty of Sciences and Technology of Coimbra University, Rua Sílvio Lima – Polo II, 3030-790 Coimbra, Portugal.
E-mail address: goreti.sales@eq.uc.pt (M. Goreti F. Sales).

https://doi.org/10.1016/j.microc.2023.109640
Received 30 July 2023; Received in revised form 4 November 2023; Accepted 9 November 2023
Available online 10 November 2023

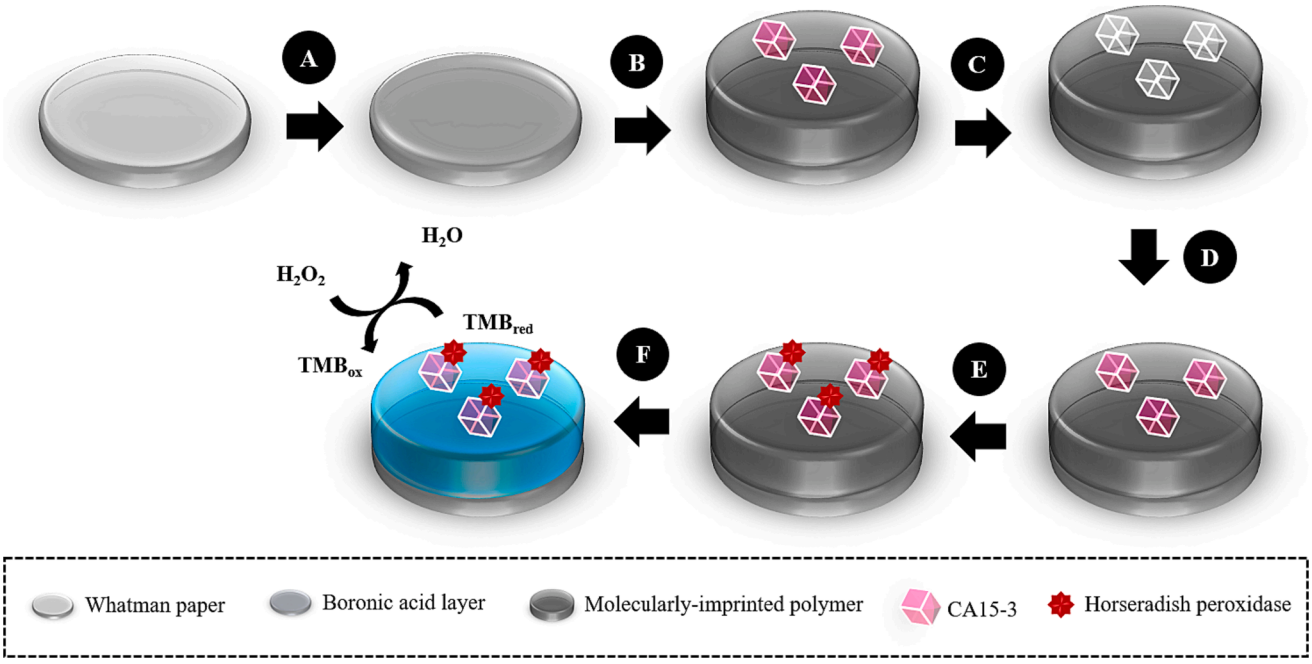

Fig. 1. Schematic representation of the sensor construction. Production of a first layer of polymerization with 3-APBA (A), production of MIP (B), removal step (C), rebinding step (D), HRP incubation (E), and color development with TMB solution (F).

diagnostic platform for biomarker detection, especially in resource-limited settings [15,19–22]. In terms of readout, various enzymes and substrates can be used in ELISA protocols, with horseradish peroxidase (HRP) in combination with 3,3′,5,5′-tetramethylbenzidine (TMB) being the most commonly used [18,23].

Since P-ELISA also uses natural antibodies to detect target biomarkers, there is room for further improvement. Natural antibodies are expensive and unstable biological compounds [24,25], which can be replaced by biomimetic analogues produced using molecularly imprinted polymers (MIPs) [16]. MIPs were originally developed for sample purification and pre-concentration of analytes, but they are also used as recognition elements for various biomarkers [17,26]. Their recognition ability is due to the complementary cavities formed during their production and allows their use as replacements for natural antibodies in ELISA, leading to biomimetic enzymatic immunoassays (B-ELISA). MIPs as alternatives to natural receptors can help overcome these drawbacks by improving sensor performance, shortening reaction time and increasing selectivity and sensitivity [26].

The first B-ELISA was published in 2000 [27]. It is cheaper, more stable and easier to produce, and has lower batch-to-batch variability than conventional ELISA approaches [2,24,28]. Various approaches have been used to integrate MIPs into ELISA assays. These include direct polymer growth on the substrate, including 96-well microplates [1] or paper substrates [16,24,29–32], or fabrication of MIP nanoparticles to coat the substrates [28].

In general, paper is a versatile substrate for the growth and immobilisation of MIPs [24], and the inclusion of MIPs as recognition elements in paper analytical devices (PADs) has led to new advances in low-cost and highly selective analytical devices [26]. Paper-based MIPs have been developed for various molecules (e.g. disease biomarkers [31], metal ions [16], pesticides [29] or pollutants [33]), with colorimetry being the main detection mode. Colour detection offers a simple visual readout that can provide qualitative or semi-quantitative data. Quantitative data is also possible, although colorimetric detection usually has low sensitivity and some non-specific adsorption [26].

This paper therefore presents a B-ELISA method for the detection of CA15-3, combining traditional ELISA (detection method) with MIP (detection element) and paper as substrate.

2. Experimental

2.1. Reagents and solutions

All chemicals employed in the present work were of analytical grade and water was ultrapure Milli-Q laboratory grade.

Sodium phosphate dibasic dihydrate and sodium chloride (NaCl) were acquired from Panreac (Spain). Sodium dihydrogen phosphate dihydrate was from Scharlau (Australia), while sodium hydroxide (NaOH) was sourced from EKA (Brazil). 3-Aminopropyltriethoxysilane (APTES) and 3-aminophenylboronic acid monohydrate (3-APBA) 98 % were both from Acros Organics (United States). As chromogenic substrate we relied TMB liquid Substrate System for ELISA and HRP (275 U mg^{-1}) from Sigma Aldrich (Germany). Dopamine, in the form of 3-hydroxytyramine chloride was purchased from Merck (Germany). Ammonium persulfate (APS) was acquired from Analar Normapur (Belgium). *N,N,N',N'*-Tetramethyl-ethylene diamine ≥ 99 % (TEMED) was obtained from Fisher Chemical (United States). Triethoxyphenylsilane (TEPS) < 98 % was acquired from Fluka (United States). Hydrogen peroxide (H_2O_2) 35 % was purchased from Labchem (United States). Absolute ethanol 99.8 % was purchased from Riedel-de-Haën (United States).

Whatman® quantitative filter paper (ash-free, grade 40, 110 mm diameter, 210 μm thickness, 8 μm pore size), from Sigma Aldrich (Germany), was used as substrate.

CA15-3 from human host (reference MBS536585) was purchased from MyBioSource (United States). The detection antibody (recombinant monoclonal antibody against MUC1 labelled with HRP, reference EPR1023) was purchased from Abcam (United Kingdom).

Stock solutions of proteins and antibodies were prepared in phosphate buffer (PB, 0.081 M Na_2HPO_4 and 0.019 M NaH_2PO_4, pH = 8.5).

2.2. Apparatus

Scanning electron microscopy (SEM) and thermogravimetric analysis (TGA) were used to characterize modified cellulose paper. SEM Images were acquired on FEI Quanta 400FEG ESEM/EDAX PEGASUS X4M instruments with gold sputter coating. TGA measurements were

performed with ≈1.5 mg of sample using a platinum holder from 30 to 1000ºC under a nitrogen atmosphere of 40 mL min^{-1}.

A homemade darkroom (19 cm width × 13.5 cm height × 13.5 cm depth) with a light-emitting diode strip (LED) (high luminosity, 4000 K, 50/60 Hz, DC12V) covering the four sides of the chamber was used for image acquisition.

2.3. Methodologies

The complete process of synthesis and detection of the protein consists of 6 main steps and is shown in Fig. 1. Before the imprinting step, the cellulose Whatman® paper was washed and functionalized. Then 3-APBA was polymerised on the surface of the paper (Fig. 1A) to react with the glycosylated CA15–3 protein. In the imprinting stage, the polydopamine layer is formed by polymerization of dopamine in the presence of CA15-3 (MIP) or in its absence (NIP) to produce a control material (Fig. 1B). The template was removed (Fig. 1C) and CA15-3 was allowed to bind the formed cavities (Fig. 1D). For the colour development, the HRP was incubated (Fig. 1E), adsorb to the proteins present and then the substrate TMB was allowed to react with H_2O_2 (Fig. 1F).

2.3.1. Synthesis of the biomimetic material

Prior to MIP production, the papers were first washed to remove impurities and functionalized to obtain functional groups. A circular Whatman® filter paper (area ≈ 95 cm^2) was immersed in H_2O_2 (5 M) for 2 h in a horizontal shaker. It was then soaked in water to remove unreacted products. A silane coupling technique was then used by immersing the paper in 50 mL of a 10 % silane mixture (APTES:TEPS, 1:1) prepared in absolute ethanol for 2 h at room temperature in a horizontal shaker. The paper was then thermally treated at 80 °C for 2 h. It was then rinsed with ethanol to remove unbound silanes and dried again. It was then stored in a desiccator until use.

After the washing and functionalization steps, the cellulose paper was cut into 8 mm circles with a hole punch and modified with poly-APBA by polymerization of the monomer APBA (1.0×10^{-4} M) using APS (1.0×10^{-6} M) and TEMED (1.0×10^{-6} M) as catalysts. These components were mixed in equal proportions and incubated on the paper circles for 2 h at room temperature in 48-well plates in a horizontal shaker. Each paper was washed with 3 mL PB (pH = 8.5) and dried at 37 °C for 15 min. MIPs were then prepared using CA15-3 as the template molecule, dopamine as the functional monomer, and TEMED and APS as catalysts. A solution containing dopamine (1.0×10^{-4} M) and CA15-3 (at a final concentration of 100 U mL^{-1}) was incubated on a small vial for 1 h with stirring and protected from light. During this step, the protein was bound to the APBA layer with its boron groups (on the outer surface) and vicinal hydroxyl groups of the glycoprotein. Then a solution containing APS and TEMED (1.0×10^{-6} M) was added to the vial and stirred for another hour. In parallel, a NIP was prepared. This final mixture was placed on paper filter circles in a 48-well plate and incubated for one hour at 25 °C with horizontal shaking to obtain a uniform polydopamine film around the paper substrate. Then, polymerization was continued for another 2 h without shaking. Finally, the papers were washed with PB to remove unreacted components and dried at 37 °C for 15 min. All solutions used for the polymerization mixture were freshly prepared and purged with nitrogen.

To remove the template, the NIPs and MIPs were incubated with sodium chloride (0.1 M) [34] for 2 h with horizontal shaking to allow imine cleavage. Then, the papers were washed with PB and left in the wells with PB for 1 h. Finally, the obtained MIPs with specific binding sites for CA15-3 were washed with PB and dried at 37 °C for 15 min.

2.3.2. Colorimetric protein detection

Under the optimized experimental conditions, the calibration assays were performed with 5 μL CA15-3 antigen standards (from 3 to 1000 U mL^{-1}) prepared in PB, pH = 8.5. The standards were added to the paper filters and incubated at 37 °C for 10 min. As a negative control, PB was added to a paper filter instead of CA15-3 to obtain a background signal. After incubation, the papers were washed with PB to remove unbound target protein and dried at 37 °C for 15 min.

In the final step of sensor construction and before color development by adding a chromogenic substrate, incubation with HRP is essential because it reduces hydrogen peroxide and oxidizes TMB, resulting in a blue color. Since the optimum pH of HRP is 7 [35] and we intend to work at physiological conditions, PB with a pH of 7.4 was used to prepare the HRP solutions. In this step, 5 μL of HRP solution (50 μg mL^{-1}) was incubated at 37 °C for 10 min. Subsequently, the papers were washed with PB and dried at 37 °C for 15 min.

A ready-to-use redox indicator solution of TMB (150 μL) was added to each paper in a 48-well plate. Let them react in the dark for 5 min. The papers were removed from the plate, the excess reagent was removed with absorbent paper, and the images were immediately captured in the homemade darkroom.

2.3.3. Real samples assay

To test the developed sensor in the presence of real samples, CA15-3 standards (from 3 to 1000 U mL^{-1}) were added to aliquots of fetal bovine serum using a 1000-fold dilution of the serum and incubated on the sensing paper circles.

2.3.4. Selectivity assay

The selectivity of the sensor was evaluated by incubating various interfering molecules that may be present in human serum samples. These include CA15-3 (250 U mL^{-1}) plus CEA (0.25 ng mL^{-1}), CA15-3 (250 U mL^{-1}) plus CA-125 (0.35 U mL^{-1}), CA15-3 (250 U mL^{-1}) plus glucose (1 mg mL^{-1}) and CA15-3 (250 U mL^{-1}) plus IgG (0.1 mg mL^{-1}), prepared in PB, and incubated on the sensor surface.

2.3.5. Analysis of results

To obtain quantitative results, images were analysed using ImageJ software. Several parameters were evaluated, and the average value of each parameter was transferred to an Excel workbook for further analysis. The YIQ system was used, where Y represents luminance and I and Q represent chrominance. The Y and Q channels were chosen because they are best suited to describe the absence/presence of the protein, being proportional to its concentration. Y is given by the equation Y = 0.229R + 0.587G + 0.114B and represents the grey scale. Q is given by the equation Q = 0.211R-0.523G + 0.312B [36] and represents the quadrature. R stands for red coordinates, G for green and B for blue coordinates.

During the optimisation steps, the difference between the Q values of NIP and MIP control (incubated with buffer) and the Q values of NIP and MIP incubated with CA15-3 was calculated. The condition where $MIP_{control}$-$MIP_{CA15\text{-}3}$ gives a higher value than $NIP_{control}$-$NIP_{CA15\text{-}3}$ was selected and used for further experiments.

3. Results and discussion

3.1. Characterization techniques

3.1.1. TGA analysis

Modification of cellulose paper substrates with sensor materials was evaluated by thermal degradation at TGA (Figure S1). As expected, the degradation profile of the cellulose paper shows a maximum degradation rate after 320 °C, leaving a residual solid of 5.6 % at 500 °C. The addition of silanes to the cellulose substrates changes the thermal stability of the material, as silanes remain stable at higher temperatures. This reduces the percentage of the material that can be subjected to degradation, leaving a residual amount of 18.7 % at 500 °C. The subsequent steps lead to the formation of MIP or NIP materials, including poly-APBA and polydopamine on the silane-cellulose composite, which in the case of MIP also contains CA15-3. Overall, the MIP and NIP polymer layers are unstable and undergo thermal degradation mainly at

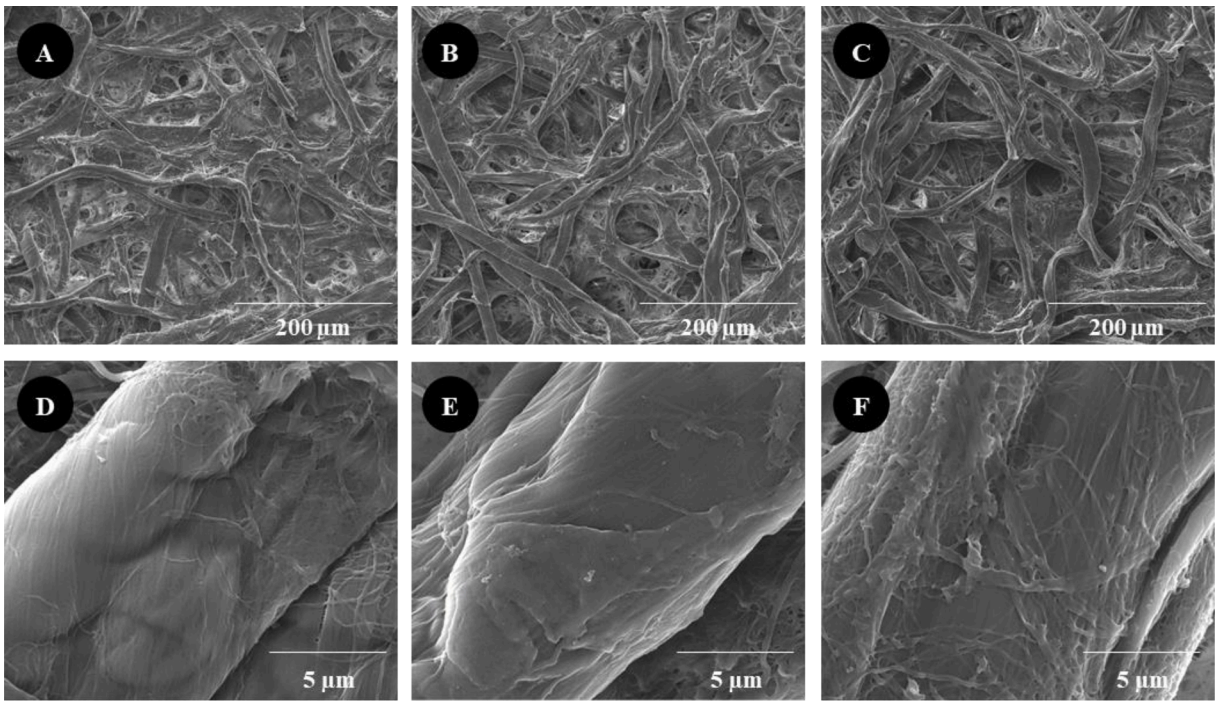

Fig. 2. SEM images of bare paper (A), NIP (B) and MIP (C) with 500 × magnification and bare paper (D), NIP (E) and MIP (F) with 15000 × magnification.

temperatures between 275 °C and 365 °C, which is accompanied by the decomposition of the cellulose materials. The fact that the degradation profile of all samples was similar agrees well with the similar chemical composition of all sensor materials and the fact that CA15-3 is present only at an extremely low percentage. Nevertheless, it is important to emphasize that the NIP sensor had a higher weight loss before template removal than the MIP with template. This essentially indicates that the polymer film NIP was formed to a higher extent because CA15-3 hindered the polymerization of the polydopamine film on the MIP, justifying the lower residual amount of NIP (11.3 % at 1000 °C) corresponding to the pure silane composition. Removal of CA15-3 from the MIP film changed the residual amount of MIP from 15.4 to 18.1 %, confirming the presence of the protein. However, the same procedure used to remove NIP resulted in a higher percent weight loss, with the residual amount increasing from 11.3 to 17.9 %. Since NIP does not contain protein to be removed, this change is likely due to the loss of the polymeric network that was not firmly attached to the sensor film. In general, the TGA information confirms the formation of the imprinted film and the effects of removal on the modified cellulose substrates, resulting in sensor materials that contain a similar percentage of polymer as the silane/cellulose composite.

3.1.2. SEM analysis

The morphology of the bare and modified cellulose substrates was characterized using SEM. Fig. 2 shows magnification images of the cellulose paper showing the typical microfibers of cellulose (Fig. 2A), which were also modified with polydopamine in the form of NIP (Fig. 2B) or MIP (Fig. 2C). The images show that the cellulose fibers were coated with polydopamine during the polymerization step, resulting in an increase in fibre diameter (Fig. 2B and Fig. 2C) compared to the bare cellulose separator (Fig. 2A). Higher magnification images show the polydopamine fibers and the rough polymeric surface in MIP (Fig. 2F) compared to bare cellulose (Fig. 2D) and to NIP (Fig. 2E), which is still smooth [29]. This roughness suggests that the presence of the template on MIP led to a different structural polymer growth. Nevertheless, the imprinted cavities on the MIP cannot be observed because the dimensions of these binding sites are below the resolution limit of the technique.

3.2. Synthesis of the biomimetic material

The biomimetic material was assembled as shown in Fig. 1, where a cellulose substrate was modified with silane chemistry, resulting in the interaction of the template with boronic acid and subsequent polymerization with dopamine to form the MIP layer.

An important aspect of any chemosensor is reproducibility, which depends first on the homogeneity of the starting material. Therefore, all paper substrates were washed with H_2O_2 before any further modification; H_2O_2 is a strong oxidizing agent that is said to oxidize impurities, increasing their water solubility in water. It also adds hydroxyl groups to the paper surface, which helps to increase the efficiency of subsequent chemical modifications with involving covalent hydroxyl bonds (as in silane chemistry) [16]. Physical adsorption would also be possible as an immobilization technique for any intended biological recognition element, but desorption of the molecules may occur during the washing steps. Therefore, cellulose was modified with silane chemistry by incubating the paper in silanes. Binding to the vicinal hydroxyl groups of the cellulose (treated with H_2O_2) and crosslinking through the porous structure of the cellulose provided stable chemistry of the silane/cellulose matrix [22,37].

Next, 3-APBA was incubated on the silane/cellulose composite followed by the protein (in the case of the MIP), to undergo the reversible reaction between boronic acid (in 3-APBA) and the *cis*-diol groups (in glycoproteins) [38]. This stage corresponds to the formation of a template monomer complex in a pre-polymerization solution, giving rise to a cyclic bromate ester. This ester is easily reversed by a change in pH/ions, releasing the protein as needed. The stability and suitability of this complex is critical, as this stage establishes the functional groups to which CA15-3 will bind after contact with the MIP in the sample.

The subsequent addition of a monomer/cross-linker and an initiator allowed the formation of the MIP film [26]. In this work, dopamine was considered as the monomer. It is a small molecule containing catechol and amine functional groups that self-polymerize in a weak alkaline pH [39]. Its polymerization is based on the oxidation of catechol group to quinone and further reaction with amine groups and other catechols and quinones, allowing the formation of a biocompatible and hydrophilic polymeric film. This polymer is highly reactive towards amine and thiol

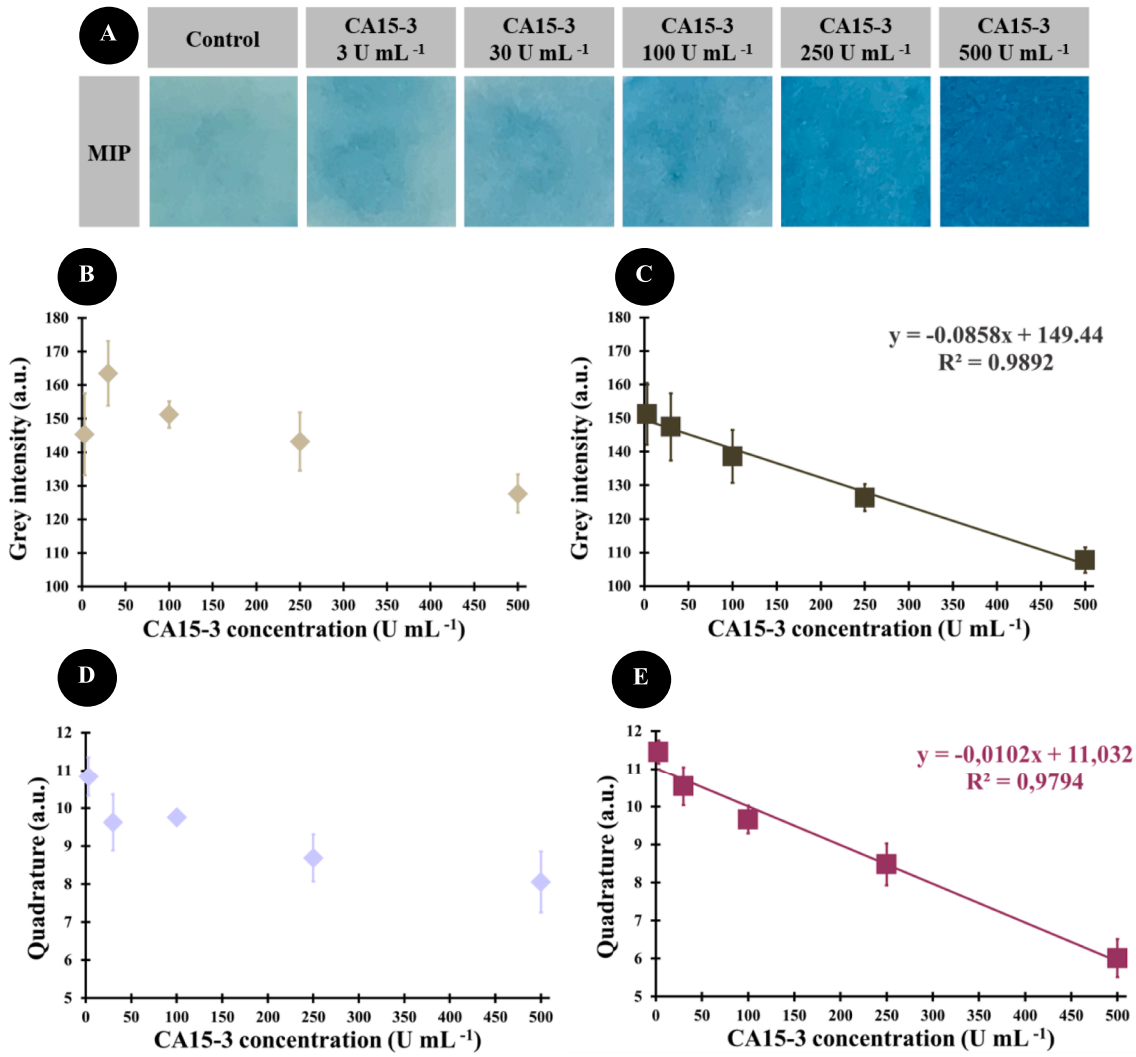

Fig. 3. Photographs of buffer calibration in MIP (A). Calibration curve based on grey intensity for NIP (B) and MIP (C). Calibration curve based on quadrature values for NIP (D) and MIP (E).

groups, which has advantages for covalent binding of target biomolecules for sensing purposes [40]. To our knowledge, the first polydopamine-based MIP was reported for nicotine sensing [41], but since then dopamine has been used in the preparation of MIPs as recognition elements for sensing of macromolecules, including proteins [40].

Removal of the template was the next step, a critical step in molecular imprinting. Efficient template removal should be performed to create the imprinted sites and allow subsequent rebinding of CA15-3 present in the sample. In addition, residual template molecules should be minimized as they are responsible for background signals [1]. Template removal was optimised by incubating NIPs and MIPs under different conditions that affect the reaction between the diol and phenylboronic acid and the conformation of the protein, while the effects on the polymer surface should be minimal. In this work, water [42], sodium chloride (0.1 M) [34], acetic acid (10 %) and sodium dodecyl sulphate (SDS, 1 %) [43] or acetic acid (3 %) and Tween-20 (0.1 %) [44] were tested, under the same experimental conditions (temperature and time). This study was made by checking how the colour of the MIP/NIP sensor paper changes between the control solution and the CA15-3 standard solution of 2000 U mL^{-1} to check the effect of removal conditions upon the sensitivity of the system. The collected images and the analytical output are shown in Figure S2. The results showed that the use of a detergent with acetic acid was undesirable, and the use of water or sodium chloride gave similar results, but with the naked-eye, sodium chloride (ΔMIP-NIP = 2.90) was slightly better than water (ΔMIP-NIP = 2.58), due to the greater differenced between the results of the control and the protein detection.

3.3. Colorimetric protein detection

The presence of CA15-3 was detected by a color change from colorless to blue because the incubation of HRP was followed by addition of a ready-to-use peroxidase substrate with TMB. The more intense the blue coloration was, the more HRP was bound to the sensor surface. This meant that HRP was bound to CA15-3 by nonspecific protein–-protein interactions. This also meant that this HRP-biomarker interaction was more intense than any interaction of HRP with polydopamine. Because this interaction was nonspecific, a larger amount of HRP would also result in color development because it binds to different sites on the sensor than the protein CA15-3. Therefore, the best experimental conditions should be optimized.

This principle was confirmed by testing different conditions for color development, as shown in Figure S3. Incubation of a TMB solution in PB on the sensor papers did not result in color development, either on NIP or on the MIP. The same was true for the sensor paper incubated with CA15-3 standard solution (1000 U mL^{-1}), which remained colorless. This indicates that the peroxidase substrate is stable with TMB and that

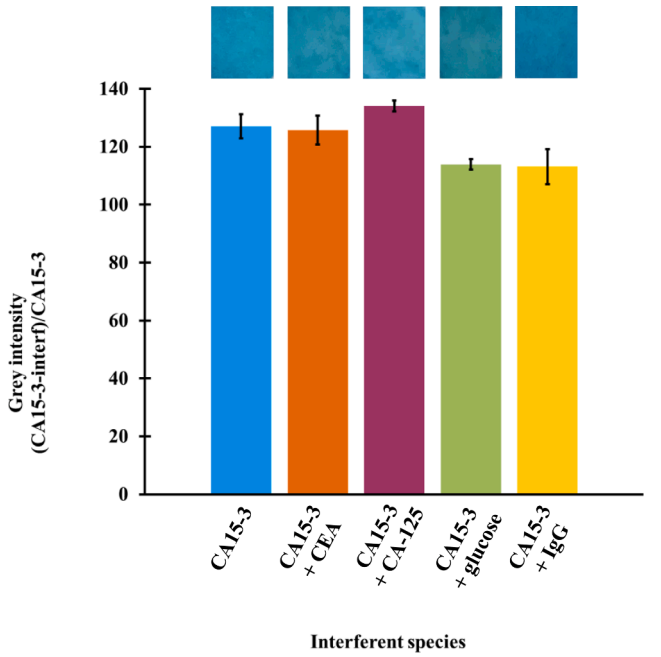

Fig. 4. Images and the respective bar chart of selectivity study based on comparison of the response of CA15–3 with different interferent species.

this substrate is not oxidized in the absence of HRP. As with conventional ELISA methods using antibodies, incubation of an antibody labelled with HRP was also attempted for CA15-3. It showed a good response with a higher value for ΔMIP than for ΔNIP, but this condition also gave high background signals. This was certainly due to the non-specific adsorption of the antibody to the polymeric material, since the epitope region of the antibody corresponds to only a small portion of the antibody and the control assays do not contain CA15-3. This was also confirmed by the more intense colour in the control assay of NIP (compared with MIP), in which CA15-3 was not present. This confirms that the MIP surface is less susceptible to non-specific adsorption. The higher color intensity of the MIP signals compared with the signals from NIP in the presence of CA15-3 proves the selective response of the MIP surface to CA15-3. Incubation of HRP alone (5 μg mL^{-1}), not in combination with an antibody, was subsequently tested. This condition resulted in a significant decrease in background signal compared to antibody binding, as no color was obtained in controls. MIP incubated with CA15-3 also showed a good (color intensive) response, which was also significantly higher than the response obtained with NIP. Increasing the amount of HRP (to 50 μg mL^{-1}) showed a very weak response on the MIP control, but the signal from the paper incubated with CA15-3 also had a blue colour. Since the ΔMIP/ΔNIP ratio is higher at the highest HRP concentration, the following tests were performed with 50 μg mL^{-1} HRP.

From another point of view, the volume of the solution used was important for the homogeneity of the sensor surface and the sensitivity of the response, as shown in Figure S4. In the previous tests, 3 μL CA15-3 solution (or buffer) and then 3 μL HRP solution were incubated on each paper circle. The results showed that only high concentrations of CA15-3 could lead to color development under these conditions and that no color was visible to the naked eye at lower concentrations. For this reason, higher volumes (4 and 5 μL) were tested. Incubation of 4 μL or 5 μL CA15-3 and HRP solutions resulted in an increase in colorimetric reaction intensity with increasing concentration of CA15-3. It was also found that not only MIPs can also recognize lower concentrations of this protein, but also NIPs can adsorb some targets. However, the recognition capacity of the MIP surface is obviously greater than the adsorption that occurs on NIPs. Five microliters were selected for further investigation because this gave the best linear response, as shown in Figure S4 (B to C). Under this condition, the quadrature signal of the sensor was saturated for concentrations > 500 U mL^{-1}, which by far includes CA15-3 levels > 30 U mL^{-1}, which are clinically important in breast cancer.

3.4. B-ELISA paper-sensor calibration

Fig. 3 shows the images of the paper sensors incubated in different concentrations of CA15-3, from 3 to 500 U mL^{-1}, in buffered solutions. The average points obtained from triplicate measurements of each data point were plotted against grey intensity or Quadrature. The error bars included correspond to the standard deviation (SD). The linear regression equation of the MIP was grey intensity = -0.0858 × CA15-3 U mL^{-1} + 149.44 (R-squared 0.9892) or Quadrature = -0.0102 × CA15-3 U mL^{-1} + 11.032 (R-squared 0.9794). The NIP showed no linear response.

3.5. Selectivity

Selectivity is a crucial parameter to be investigated when evaluating the performance of a biosensor to assess whether it can be used in real-world conditions. The selectivity assay was performed by incubating CA15-3 solutions prepared alone or in the presence of a possible interfering substance. Assays were performed in triplicate and data were expressed as mean ± SD. Fig. 4 shows the mean values in terms of percent signal change compared with CA15-3 alone. CEA (1 %) and CA −125 (5.5 %) resulted in small differences in grey scale compared with the effect of glucose (10.4 %) and IgG (11 %). Overall, the effect of the four interfering species tested in this assay was negligible with error values equal to or below 11 %. The results show that the MIP surface has high selectivity for CA15-3 compared to the interfering molecules tested. This is mainly due to the presence of the imprinted cavities for CA15-3. These results suggest that these sensors could be used to detect CA15-3 in complex matrices.

3.6. B-ELISA paper-sensor in serum samples

Fig. 5 shows the sensor response for detection of CA15-3 in fetal bovine serum. Calibrations were performed in a background medium of serum to achieve an analytical level of communication well matched to the composition of the sample. For this purpose, the standard samples of CA15-3 contained real serum in their composition. As with the buffered solutions, calibrations were performed in triplicate and data are reported as mean ± standard deviation. The overall behaviour showed a linear trend for both grey-scale and quadrature values as a function of CA15-3 concentration (U mL^{-1}), corresponding to grey-scale = -0.0956 × CA15-3 U mL^{-1} + 158.05 (R square 0.997) and quadrature = -0.0098 × CA15-3 U mL^{-1} + 11.006 (R square 0.9903). Compared with the experiments with buffer, the slope values were similar, as was the range of linear response. The results obtained indicate that this sensor can be used to detect CA15-3 in serum samples.

4. Conclusions

The combination of MIPs, paper and ELISA has already been reported, but only for small molecules [16,24,29–31]. As we know, no one has yet used this for the detection of (glyco)proteins (Table 1). Nevertheless, several biosensors for CA15-3 have been described using different recognition elements and transduction systems. Most of the mentioned works have LODs between 0 and 2 U mL^{-1} [6–11,13], but some of them can actually reach a very low LOD, such as the work by Wu et al. (LOD = 2.56 × 10^{-5} U mL^{-1}) [12]. Despite the high sensitivity of this work, the fluorescence signal emitted by the sensor requires a fluorometer, which may be a limitation. In addition, some of them report very narrow linear ranges (e.g., 0.1–20 U mL^{-1} [7], 0.25 to 10 U mL^{-1} [11], 0.25–14 U mL^{-1} [12]), which might not be very useful in clinical practice because the CA15-3 cut-off is 30 U mL^{-1}.

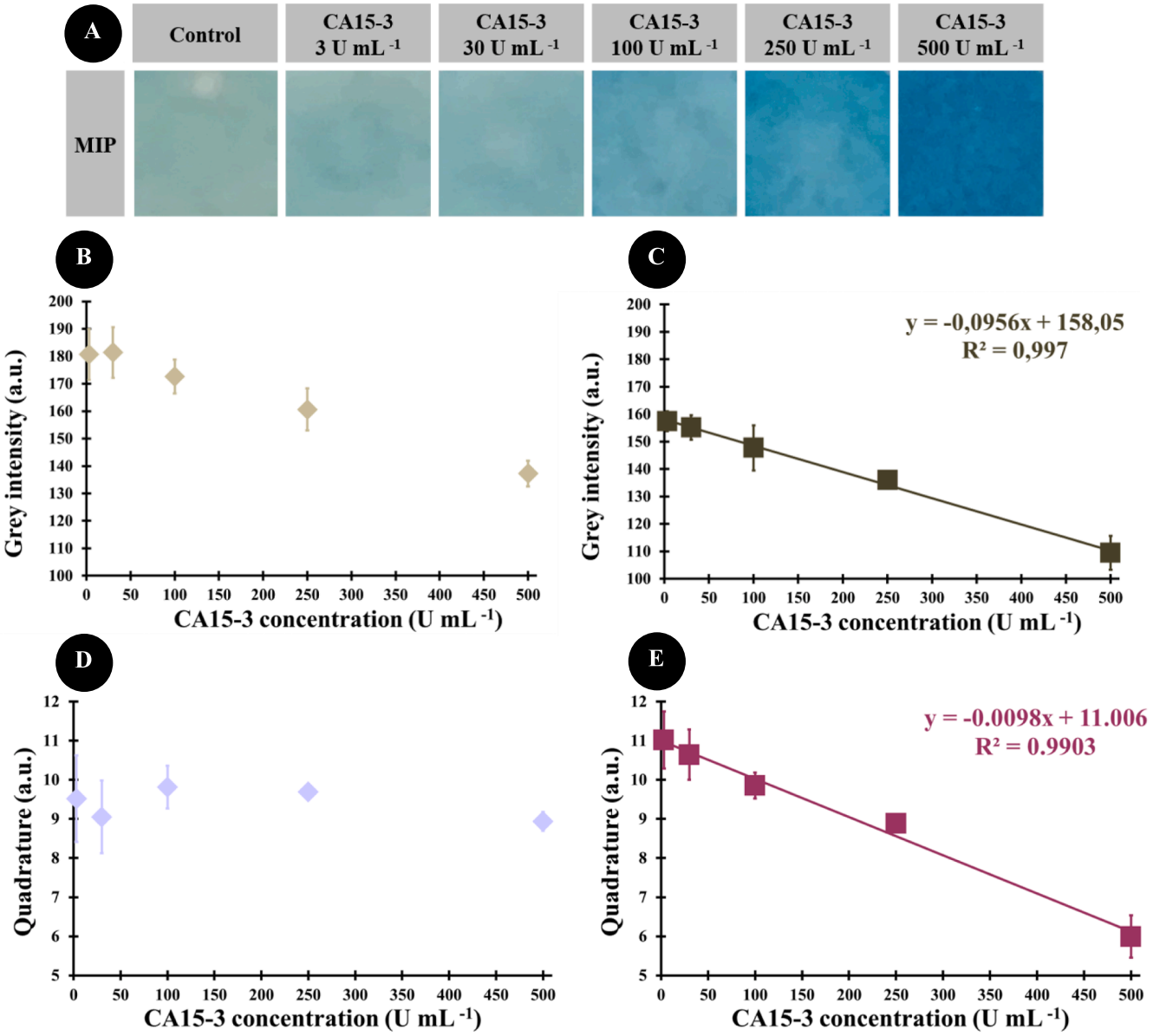

Fig. 5. Photographs of fetal bovine serum calibration in MIP (A). Calibration curve based on grey intensity for NIP (B) and MIP (C). Calibration curve based on quadrature values for NIP (D) and MIP (E).

This work demonstrates that it is possible to assemble a MIP material on a paper substrate that can selectively bind target proteins of interest, in this case CA15-3. This highlights the increasing attention given to MIP-based sensors, as they are easy to fabricate, robust, stable, and inexpensive. Their incorporation into PADs provides a versatile tool that can be used in a variety of situations. The use of an ELISA-like system was also introduced presented as a simple approach to identify the presence of bound CA15-3. The results confirmed the need for HRP, but the presence of an antibody for this purpose (as within conventional ELISA) was not required. The paper-based B-ELISA showed good linear correlation over a wide range of concentrations (3 to 500 U mL^{-1}) and the selectivity of the developed sensor was very high.

The advantages of using cellulose paper as ELISA substrate for CA15-3 were already demonstrated in a previous work [6], but antibodies were used as recognition elements. In the present work, we maintain the choice of cellulose paper as substrate and colorimetric substrate for the transduction system, but we would like to highlight the outstanding advantages of using a MIP instead of an antibody as detection element. If we compare the traditional ELISA (in 96-wells) with the P-ELISA, we can find that the latter has outstanding advantages such as portability, ease of use, and rapid response due to the use of paper as a substrate and is also more cost-effective because it does not require the use of natural antibodies. In terms of analytical performance, both works achieved very similar linearity (R2≈0.99) when the sensors are calibrated with serum samples. Despite the advantages, the B-ELISA takes more time, which is due to the steps associated with the MIP design. The proposed approach can be easily extended to other glycoproteins that need to be monitored at the point-of-care, as a screening test in the physician's office or in countries that do not have easy access to healthcare facilities.

CRediT authorship contribution statement

Mariana C.C.G. Carneiro: Investigation, Validation, Data curation, Writing – original draft, Visualization. **Lígia R. Rodrigues:** Conceptualization, Validation, Data curation, Writing – review & editing. **Felismina Moreira:** Validation, Resources, Data curation, Writing – review & editing, Visualization, Project administration. **M. Goreti F. Sales:** Conceptualization, Methodology, Resources, Writing – review & editing,

Table 1
Published works for molecular imprinting polymers combined with colorimetric detection on a paper substrate.

Target	Analyte recognition	Colorimetric detection	Linear range	Limit of detection	Reference
Bisphenol A	$ZnFe_2O_4$-@MIP membranes	TMB	0.01 to 1 μM	6.18 nM	[29]
Tetrabromobisphenol A	Copper-based metalorganic framework (MIP/HKUST-1)	TMB	0.01 to 10 ng g^{-1}	3 pg/g	[30]
Sulfamethoxazole	MIP	Diazotization reaction + naphthyl ethylenediamine dihydrochloride	0 to 3 and 3 to 10 ppm	0.24 ppm	[33]
Thiacloprid	MIP-capped metal–organic frameworks	TMB	0.1 to 1.2 and 1.2 to 10 μM	0.04 μM	[45]
Kanamycin	metal–organic framework/molecularly imprinted polymer chip (FZS@CPBA@MIP)	ninhydrin-aminoglycoside antibiotic	0.1 to 25 mg L^{-1}	4.69 μg L^{-1}	[46]
Carbaryl	Biomimetic ELISA	TMB	0.001 to 1 mg L^{-1}	0.007 mg L^{-1}	[24]
	Mesoporous silica-platinum nanoparticles coated with a molecularly imprinted polymer (MSN-PtNPs@MIP)	TMB	0.002 to 20.00 mg kg^{-1}	15 ng g^{-1}	[47]
Cd (II)	Ion imprinted polymers (IIPs)	dithizone	1 to 100 ng mL^{-1}	0.4 ng mL^{-1}	[16]
	MIP	TMB	0 to 300 ppb	0.1 ppb	[48]
17β-estradiol	MIP grafted paper	chromogenic substrate	–	0.25 μg L^{-1}	[31]
CA15-3	Biomimetic ELISA	TMB	3 to 500 U mL^{-1}	3 U mL^{-1}	This work

Funding acquisition.

Declaration of Competing Interest

The authors declare that they have no known competing financial interests or personal relationships that could have appeared to influence the work reported in this paper.

Data availability

No data was used for the research described in the article.

Acknowledgements

This study was supported by the Portuguese Foundation for Science and Technology (FCT) under the scope of the strategic funding of UIDB/04469/2020 unit. Authors also acknowledge FCT for funding the PhD grant reference SFRH/BD/131959/2017.

Appendix A. Supplementary data

Supplementary data to this article can be found online at https://doi.org/10.1016/j.microc.2023.109640.

References

[1] X. Bi, Z. Liu, Facile Preparation of glycoprotein-imprinted 96-well microplates for enzyme-linked immunosorbent assay by boronate affinity-based oriented surface imprinting, Anal. Chem. 86 (1) (2014) 959–966, https://doi.org/10.1021/ac403736y.
[2] S. Ansari, S. Masoum, Molecularly imprinted polymers for capturing and sensing proteins: current progress and future implications, TrAC Trends Anal. Chem. 114 (2019) 29–47, https://doi.org/10.1016/j.trac.2019.02.008.
[3] M.J. Duffy, D. Evoy, E.W. McDermott, CA 15–3: uses and limitation as a biomarker for breast cancer, Clin. Chim. Acta 411 (23) (2010/12/14/ 2010,) 1869–1874, https://doi.org/10.1016/j.cca.2010.08.039.
[4] B. Hirata, J. Massayo Maeda Oda, R. Guembarovski, C. Ariza, C. Oliveira, M. Watanabe, Molecular Markers for Breast Cancer: Prediction on Tumor Behavior. (2014), 513158.
[5] R. Hong *et al.*, "A Review of Biosensors for Detecting Tumor Markers in Breast Cancer," *Life*, vol. 12, no. 3, doi: 10.3390/life12030342.
[6] M.C.C.G. Carneiro, L.R. Rodrigues, F.T.C. Moreira, M. Goreti, F. Sales, Paper-based ELISA for fast CA 15–3 detection in point-of-care, Microchem. J. 181 (2022), 107756, https://doi.org/10.1016/j.microc.2022.107756.
[7] H. Li, J. He, S. Li, and A. P. F. Turner, "Electrochemical immunosensor with N-doped graphene-modified electrode for label-free detection of the breast cancer biomarker CA 15-3," *Biosensors and Bioelectronics,* vol. 43, pp. 25-29, 5/15/ 2013, doi: https://doi.org/10.1016/j.bios.2012.11.037.
[8] T.S.C.R. Rebelo, J.A. Ribeiro, M.G.F. Sales, C.M. Pereira, Electrochemical immunosensor for detection of CA 15–3 biomarker in point-of-care, Sens. Bio-Sens. Res. 33 (2021), 100445, https://doi.org/10.1016/j.sbsr.2021.100445.
[9] J.A. Ribeiro, C.M. Pereira, A.F. Silva, M.G.F. Sales, Disposable electrochemical detection of breast cancer tumour marker CA 15–3 using poly(Toluidine Blue) as imprinted polymer receptor, Biosens. Bioelectron. 109 (2018) 246–254, https://doi.org/10.1016/j.bios.2018.03.011.
[10] J.G. Pacheco, M.S.V. Silva, M. Freitas, H.P.A. Nouws, C. Delerue-Matos, Molecularly imprinted electrochemical sensor for the point-of-care detection of a breast cancer biomarker (CA 15–3), Sens. Actuators B 256 (2018) 905–912, https://doi.org/10.1016/j.snb.2017.10.027.
[11] R.S. Gomes, F.T.C. Moreira, R. Fernandes, M.G.F. Sales, Sensing CA 15–3 in point-of-care by electropolymerizing O-phenylenediamine (oPDA) on Au-screen printed electrodes, PLoS One 13 (5) (2018) e0196656.
[12] Y. Wu, et al., A fluorescent biosensor based on prismatic hollow Metal-polydopamine frameworks and 6-carboxyfluorescein (FAM)-labeled protein aptamer for CA15-3 detection, Sens. Actuators B 329 (2021), 129249, https://doi.org/10.1016/j.snb.2020.129249.
[13] J.A. Ribeiro, M.G.F. Sales, C.M. Pereira, Electrochemistry-assisted surface plasmon resonance biosensor for detection of CA 15–3, Anal. Chem. 93 (22) (2021) 7815–7824, https://doi.org/10.1021/acs.analchem.0c05367.
[14] A. Cerda-Kipper, B. Montiel, S. Hosseini, Radioimmunoassay and Enzyme-Linked Immunosorbent Assay (2018).
[15] C.-M. Cheng, et al., Paper-Based ELISA, Angew. Chem. Int. Ed. 49 (28) (2010) 4771–4774, https://doi.org/10.1002/anie.201001005.
[16] K. Huang, et al., Integrated ion imprinted polymers-paper composites for selective and sensitive detection of Cd(II) ions, J. Hazard. Mater. 333 (2017) 137–143, https://doi.org/10.1016/j.jhazmat.2017.03.035.
[17] S. Xu, Z. Xu, and Z. Liu, "Paper-Based Molecular-Imprinting Technology and Its Application," *Biosensors*, vol. 12, no. 8, doi: 10.3390/bios12080595.
[18] S. Wang, S. Xu, Q. Zhou, Z. Liu, and Z. Xu, "State-of-the-art molecular imprinted colorimetric sensors and their on-site inspecting applications," *Journal of Separation Science*, https://doi.org/10.1002/jssc.202201059 vol. n/a, no. n/a, p. 2201059, 2023/02/26 2023, doi: 10.1002/jssc.202201059.
[19] S. K. Vashist and J. H. T. Luong, "Chapter 5 - Enzyme-Linked Immunoassays," in *Handbook of Immunoassay Technologies*, S. K. Vashist and J. H. T. Luong Eds.: Academic Press, 2018, pp. 97-127.
[20] P. Bai, Y. Luo, Y. Li, X.-D. Yu, H.-Y. Chen, Study on enzyme linked immunosorbent assay using paper-based micro-zone plates, Chin. J. Anal. Chem. 41 (1) (2013) 20–24, https://doi.org/10.1016/S1872-2040(13)60620-9.
[21] J. Chi, et al., Patterned photonic nitrocellulose for pseudopaper ELISA, Anal. Chem. 89 (14) (2017) 7727–7733, https://doi.org/10.1021/acs.analchem.7b01732.
[22] X. Zhu, S. Xiong, J. Zhang, X. Zhang, X. Tong, S. Kong, Improving paper-based ELISA performance through covalent immobilization of antibodies, Sens. Actuators B 255 (2018) 598–604, https://doi.org/10.1016/j.snb.2017.08.090.
[23] L.S.A. Busa, M. Maeki, A. Ishida, H. Tani, M. Tokeshi, Simple and sensitive colorimetric assay system for horseradish peroxidase using microfluidic paper-based devices, Sens. Actuators B 236 (2016) 433–441, https://doi.org/10.1016/j.snb.2016.06.013.
[24] C. Zhang, H. Cui, Y. Han, F. Yu, X. Shi, Development of a biomimetic enzyme-linked immunosorbent assay based on molecularly imprinted polymers on paper for the detection of carbaryl, Food Chem. 240 (2018) 893–897, https://doi.org/10.1016/j.foodchem.2017.07.109.
[25] Y. Saylan, A. Denizli, Molecularly imprinted polymer-based microfluidic systems for point-of-care applications, Micromachines 10 (11) (2019) 766, https://doi.org/10.3390/mi10110766.
[26] W. Li, X. Zhang, T. Li, Y. Ji, R. Li, Molecularly imprinted polymer-enhanced biomimetic paper-based analytical devices: a review, Anal. Chim. Acta 1148 (2021), 238196, https://doi.org/10.1016/j.aca.2020.12.071.
[27] I. Surugiu *et al.*, "An enzyme-linked molecularly imprinted sorbent assay," *Analyst,* 10.1039/A908871G vol. 125, no. 1, pp. 13-16, 2000, doi: 10.1039/A908871G.

[28] J. Xu, H. Miao, J. Wang, G. Pan, Molecularly imprinted synthetic antibodies: from chemical design to biomedical applications, Small 16 (27) (2020) 1906644, https://doi.org/10.1002/smll.201906644.
[29] Q. Kong, Y. Wang, L. Zhang, S. Ge, J. Yu, A novel microfluidic paper-based colorimetric sensor based on molecularly imprinted polymer membranes for highly selective and sensitive detection of bisphenol A, Sens. Actuators B 243 (2017) 130–136, https://doi.org/10.1016/j.snb.2016.11.146.
[30] L. Zeng, et al., Colorimetric determination of tetrabromobisphenol A based on enzyme-mimicking activity and molecular recognition of metal-organic framework-based molecularly imprinted polymers, Microchim. Acta 187 (2) (2020) 142, https://doi.org/10.1007/s00604-020-4119-9.
[31] L. Xiao, Z. Zhang, C. Wu, L. Han, H. Zhang, Molecularly imprinted polymer grafted paper-based method for the detection of 17β-estradiol, Food Chem. 221 (2017) 82–86, https://doi.org/10.1016/j.foodchem.2016.10.062.
[32] S. Wang, L. Ge, L. Li, M. Yan, S. Ge, J. Yu, Molecularly imprinted polymer grafted paper-based multi-disk micro-disk plate for chemiluminescence detection of pesticide, Biosens. Bioelectron. 50 (2013) 262–268, https://doi.org/10.1016/j.bios.2013.07.003.
[33] A. Lamaoui, A. Karrat, A. Amine, Molecularly imprinted polymer integrated into paper-based analytical device for smartphone-based detection: application for sulfamethoxazole, Sens. Actuators B 368 (2022/10/01/ 2022,), 132122, https://doi.org/10.1016/j.snb.2022.132122.
[34] S.H. Ou, M.C. Wu, T.C. Chou, C.C. Liu, Polyacrylamide gels with electrostatic functional groups for the molecular imprinting of lysozyme, Anal. Chim. Acta 504 (2004) 163–166, https://doi.org/10.1016/S0003-2670(03)00531-2.
[35] G.T. Hermanson, Chapter 22 - Enzyme Modification and Conjugation, in: G. T. Hermanson (Ed.), Bioconjugate Techniques (third Edition), Academic Press, Boston, 2013, pp. 951–957.
[36] N. Ibraheem, M. Hasan, R. Z. Khan, and P. Mishra, "Understanding Color Models: A Review," *ARPN Journal of Science and Technology,* vol. 2, 2012.
[37] W. Hong, S.-G. Jeong, G. Shim, D.Y. Kim, S.P. Pack, C.-S. Lee, Improvement in the reproducibility of a paper-based analytical device (PAD) using stable covalent binding between proteins and cellulose paper, Biotechnology and Bioprocess Engineering: BBE 23 (6) (2018) 686–692, https://doi.org/10.1007/s12257-018-0430-2.
[38] Z. Liu, H. He, Synthesis and applications of boronate affinity materials: from class selectivity to biomimetic specificity, Acc. Chem. Res. 50 (9) (2017) 2185–2193, https://doi.org/10.1021/acs.accounts.7b00179.
[39] Y.-Z. Zhang, J.-W. Zhang, C.-Z. Wang, L.-D. Zhou, Q.-H. Zhang, C.-S. Yuan, Polydopamine-coated magnetic molecularly imprinted polymers with fragment template for identification of pulsatilla saponin metabolites in rat feces with UPLC-Q-TOF-MS, J. Agric. Food Chem. 66 (3) (2018) 653–660, https://doi.org/10.1021/acs.jafc.7b05747.
[40] P. Palladino, F. Bettazzi, S. Scarano, "Polydopamine: surface coating, molecular imprinting, and electrochemistry-successful applications and future perspectives in (bio)analysis," (in eng), Anal. Bioanal. Chem. 411 (1618–2650) (2019) 4327–4338, https://doi.org/10.1007/s00216-019-01665-w.
[41] K. Liu, J.-X. Wei Wz Fau - Zeng, X.-Y. Zeng Jx Fau - Liu, Y.-P. Liu Xy Fau - Gao, and Y. P. Gao, "Application of a novel electrosynthesized polydopamine-imprinted film to the capacitive sensing of nicotine," *Analytical and Bioanalytical Chemistry,* vol. 385, no. 1618-2642, 2006, doi: 10.1007/s00216-006-0489-z.
[42] A. Uysal, G. Demirel, E. Turan, T. Çaykara, Hemoglobin recognition of molecularly imprinted hydrogels prepared at different pHs, Anal. Chim. Acta 625 (1) (2008) 110–115, https://doi.org/10.1016/j.aca.2008.07.010.
[43] G. Fu, J. Zhao, H. Yu, L. Liu, B. He, Bovine serum albumin-imprinted polymer gels prepared by graft copolymerization of acrylamide on chitosan, React. Funct. Polym. 67 (5) (2007) 442–450, https://doi.org/10.1016/j.reactfunctpolym.2007.02.006.
[44] A. Bossi, S.A. Piletsky, E.V. Piletska, P.G. Righetti, A.P.F. Turner, Surface-grafted molecularly imprinted polymers for protein recognition, Anal. Chem. 73 (21) (2001) 5281–5286, https://doi.org/10.1021/ac0006526.
[45] X. Zhang, et al., Uniform stain pattern of robust MOF-mediated probe for flexible paper-based colorimetric sensing toward environmental pesticide exposure, Chem. Eng. J. 451 (2023), 138928, https://doi.org/10.1016/j.cej.2022.138928.
[46] J. Song, et al., Rapid measurement of residual kanamycin using highly specific biomimetic recognition paper-based chip, Anal. Chem. 94 (50) (2022) 17567–17576, https://doi.org/10.1021/acs.analchem.2c03932.
[47] M. Amatatongchai, et al., "Origami 3D-microfluidic paper-based analytical device for detecting carbaryl using mesoporous silica-platinum nanoparticles with a molecularly imprinted polymer shell," (in eng), 1873-3573 (Electronic), Talanta (2023), https://doi.org/10.1016/j.talanta.2022.124202.
[48] R. Attaallah, A. Amine, Highly selective and sensitive detection of cadmium ions by horseradish peroxidase enzyme inhibition using a colorimetric microplate reader and smartphone paper-based analytical device, Microchem. J. 172 (2022), 106940, https://doi.org/10.1016/j.microc.2021.106940.